Generalized formulations for aerial image based lens aberration metrology in lithographic tools with arbitrarily shaped illumination sources

Wei Liu,[1] Shiyuan Liu,[2,*] Tielin Shi,[1] and Zirong Tang[1]

[1]*Wuhan National Laboratory for Optoelectronics, Huazhong University of Science and Technology, Wuhan 430074, China*
[2]*State Key Laboratory of Digital Manufacturing Equipment and Technology, Huazhong University of Science and Technology, Wuhan 430074, China*
**shyliu@mail.hust.edu.cn*

Abstract: In the current optical lithography processes for semiconductor manufacturing, differently shaped illumination sources have been widely used for the need of stringent critical dimension control. This paper proposes a technique for in situ measurement of lens aberrations with generalized formulations of odd and even aberration sensitivities suitable for arbitrarily shaped illumination sources. With a set of Zernike orders, these aberration sensitivities can be treated as a set of analytical kernels which succeed in constructing a sensitivity function space. The analytical kernels reveal the physical essence of partially coherent imaging systems by taking into account the interaction between the wavefront aberration and the illumination source, and take the advantage of realizing a linear and analytical relationship between the Zernike coefficients to be measured and the measurable physical signals. A variety of mainstream illumination sources with spatially variable intensity distributions were input into the PROLITH for the simulation work, which demonstrates and confirms that the generalized formulations are suitable for measuring lens aberrations up to a high order Zernike coefficient under different types of source distributions. The technique is simple to implement and will have potential applications in the in-line monitoring of imaging quality of current lithographic tools.

OCIS codes: (110.5220) Photolithography; (120.0120) Instrumentation, measurement, and metrology; (220.1010) Aberrations theory; (110.4980) Partial coherence in imaging

References and links

1. H. Nomura, and T. Sato, "Techniques for measuring aberrations in lenses used in photolithography with printed patterns," Appl. Opt. **38**(13), 2800–2807 (1999).
2. H. Nomura, K. Tawarayama, and T. Kohno, "Aberration measurement from specific photolithographic images: a different approach," Appl. Opt. **39**(7), 1136–1147 (2000).
3. J. Sung, M. Pitchumani, and E. G. Johnson, "Aberration measurement of photolithographic lenses by use of hybrid diffractive photomasks," Appl. Opt. **42**(11), 1987–1995 (2003).
4. F. Wang, X. Wang, and M. Ma, "Measurement technique for in situ characterizing aberrations of projection optics in lithographic tools," Appl. Opt. **45**(24), 6086–6093 (2006).
5. B. W. Smith, and R. Schlief, "Understanding lens aberration and influences to lithographic imaging," Proc. SPIE **4000**, 294–306 (2000).
6. L. Zavyalova, A. Bourov, and B. W. Smith, "Automated aberration extraction using phase wheel targets," Proc. SPIE **5754**, 1728–1737 (2005).
7. F. Zernike, "Beugungstheorie des Schneidenverfahrens und seiner verbesserten form, der Phasenkontrastmethode," Physica **1**(7-12), 689–704 (1934).
8. H. van der Laan, M. Dierichs, H. van Greevenbroek, E. McCoo, F. Stoffels, R. Pongers, and R. Willekers, "Aerial image measurement methods for fast aberration setup and illumination pupil verification," Proc. SPIE **4346**, 394–407 (2001).
9. Q. Yuan, X. Wang, Z. Qiu, F. Wang, M. Ma, and L. He, "Coma measurement of projection optics in lithographic tools based on relative image displacements at multiple illumination settings," Opt. Express **15**(24), 15878–15885 (2007).

#132739 - $15.00 USD Received 2 Aug 2010; accepted 28 Aug 2010; published 3 Sep 2010

10. Z. Qiu, X. Wang, Q. Bi, Q. Yuan, B. Peng, and L. Duan, "Translational-symmetry alternating phase shifting mask grating mark used in a linear measurement model of lithographic projection lens aberrations," Appl. Opt. **48**(19), 3654–3663 (2009).
11. Z. Qiu, X. Wang, Q. Yuan, and F. Wang, "Coma measurement by use of an alternating phase-shifting mask mark with a specific phase width," Appl. Opt. **48**(2), 261–269 (2009).
12. Q. Yuan, X. Wang, Z. Qiu, F. Wang, and M. Ma, "Even aberration measurement of lithographic projection system based on optimized phase-shifting marks," Microelectron. Eng. **86**(1), 78–82 (2009).
13. J. K. Tyminski, T. Hagiwara, N. Kondo, and H. Irihama, "Aerial image sensor: in-situ scanner aberration monitor," Proc. SPIE **6152**, 61523D (2006).
14. T. Hagiwara, N. Kondo, I. Hiroshi, K. Suzuki, and N. Magome, "Development of aerial image based aberration measurement technique," Proc. SPIE **5754**, 1659–1669 (2005).
15. W. Liu, S. Liu, T. Zhou, and L. Wang, "Aerial image based technique for measurement of lens aberrations up to 37th Zernike coefficient in lithographic tools under partial coherent illumination," Opt. Express **17**(21), 19278–19291 (2009).
16. A. K. Wong, Resolution Enhancement Techniques, (SPIE Press, 2001).
17. F. Schellenberg, "Resolution enhancement technology: The past, the present, and extensions for the future," Proc. SPIE **5377**, 1–20 (2004).
18. M. Mulder, A. Engelen, O. Noordman, R. Kazinczi, G. Streutker, B. van Drieenhuizen, S. Hsu, K. Gronlund, M. Degünther, D. Jürgens, J. Eisenmenger, M. Patra, and A. Major, "Performance of a programmable illuminator for generation of freeform sources on high NA immersion systems," Proc. SPIE **7520**, 75200Y (2009).
19. A. Engelen, M. Mulder, I. Bouchoms, S. Hansen, A. Bouma, A. Ngai, M. van Veen, and J. Zimmermann, "Imaging solutions for the 22nm node using 1.35NA," Proc. SPIE **7274**, 72741Q (2009).
20. Y. Granik, and K. Adam, "Analytical approximations of the source intensity distributions," Proc. SPIE **5992**, 599255 (2005).
21. H. Hopkins, "On the diffraction theory of optical images," Proc. R. Soc. A **217**(1130), 408–432 (1953).

1. Introduction

With ever decreasing of feature sizes, lens aberration has become increasingly important for the imaging quality control of projection lithographic tools [1–4]. As numerical aperture (NA) of current projection lens yields to the manufacturing limit adapting to a higher resolution, it is necessary to ensure optical path tolerances on the order of several nanometers over extremely large aperture. Therefore, there is a need for the manufactures of lithographic tools to develop in situ techniques and systems to accurately measure aberrations up to the 37th or even higher-order Zernike coefficient [5–7].

Due to the advantage of lower cost and easier implementation in lithographic tools, aerial image based techniques have been widely used for the in situ metrology of lens aberrations. ASML Corporation has developed an aerial image based technique known as TAMIS (TIS at multiple illumination settings), which utilizes a TIS (transmission image sensor) built into the wafer stage for receiving the aerial image intensity of the test binary grating mark [8]. The Zernike coefficients are calculated directly from the image displacements of the mark at multiple NA and partial coherence factor σ settings through a matrix of sensitivities, which is a function of the corresponding multiple NA/σ settings. Wang et al recently reported a series of TAMIS based techniques to improve the measurement accuracy of coma and even aberrations by optimization of the test marks using phase-shifting gratings [9–12]. Although the main advantage of TAMIS and its improved techniques is to present a simplified linear model in a simple form that can be fully characterized by a matrix of sensitivities, there is no compact analytical formulation for the matrix of sensitivities itself. The matrix of sensitivities has to be carefully obtained in advance and can be only calculated by lithographic simulators or plenty of experimental data. Furthermore, the test marks used in TAMIS based techniques are orientated in 0° and 90° or additional directions of 45° and 135°, which maintain high sensitivity only to spherical, coma and astigmatism, thus are unable to measure high-order aberrations up to the 37th Zernike coefficient.

In the meantime, Nikon Corporation has proposed a Z37 AIS (aerial image sensor) technique which is able to measure aberrations up to the 37th Zernike coefficient by introducing a set of 36 binary grating marks with different pitches and orientations [13,14]. As these gratings are corresponding to 72 pupil sampling points, the wavefront aberration at each sampling point over the pupil plane can be easily obtained by the spectrum of the aerial image intensity. However, since obtaining the wavefront at each sampling point requires highly coherent illumination, the Z37 AIS technique works best with coherent sources, and is

#132739 - $15.00 USD Received 2 Aug 2010; accepted 28 Aug 2010; published 3 Sep 2010

therefore unsuitable for aberration measurement in lithographic tools under partially coherent illumination.

Recently we reported a technique for in situ metrology of lens aberrations up to the 37th Zernike coefficient under partially coherent illumination [15]. The technique involves to acquire the aerial image intensities of a set of 36 binary gratings with different pitches and orientations, and to analyze the through-focus information of the + 1st-order intensity spectrum of each binary grating mark. The Zernike coefficients for odd aberration and even aberration are easily obtained by calculating the phase shift and the axial shift of the + 1st-order intensity spectrum with two matrixes of aberration sensitivities respectively. As each of the aberration sensitivities is presented in a compact analytical formulation and can be easily calculated in advance by numerical method instead of only by a lithographic simulator, this technique leads to improved convenience for aberration metrology compared to the widely used TAMIS technique. Due to further considering the influence of the partial coherence factor on pupil sampling, this technique also overcomes the drawback of Z37 AIS technique as the latter only works best under the condition of highly coherent illumination. It is noted that for the first demonstration of this technique we just used a conventional source with a circular top-hat distribution as the effective illumination source, which is simply characterized by the partial coherence factor. However, a variety of off-axis illumination configurations, such as annular, dipole, and quadruple sources, which can no longer be simply characterized by only one coherence factor, have been widely used for resolution enhancement [16,17], and most recently freeform illumination sources were even introduced to help extend the resolution limit of current high NA tools [18,19]. In addition, the actual illumination sources used in real-world lithographic tools always deviate significantly from a simple top-hat distribution, instead they are typically expressed as a smooth function with variable intensity distributions such as Gaussian fall-off [20]. Therefore, it is highly desirable to further extend our technique into a generalized one that is suitable not only for circular top-hat sources, but also for arbitrarily shaped illumination sources with spatially variable intensity distributions.

In this paper, we extend our technique with generalized formulations suitable for arbitrarily shaped illumination sources by further derivation of the analytical aberration sensitivities based on the Hopkins theory of partially coherent imaging. The aberration sensitivities can be categorized into odd and even types, each of which is presented as an aberration sensitivity function determined by independent variables of the Zernike order, source distribution and pupil position. With a set of Zernike orders, these aberration sensitivities can be considered as a set of analytical kernels which succeed in forming a sensitivity function space for aberration measurement under arbitrarily shaped illumination sources. By the expansion of measurable information of through-focus images into the sensitivity function space, Zernike coefficients up to the 37th order can be conveniently obtained by the least-square method. A variety of mainstream illumination sources with spatially variable intensity distributions were input into the PROLITH to conduct the simulation work in order to validate the proposed generalized formulations.

2. Theory

We introduce an effective source function $J(\mathbf{r}_c)$ to accurately characterize an arbitrarily shaped source with spatially variable intensity distributions, where $\mathbf{r}_c$ is the normalized pupil vector that can be expressed in normalized polar coordinates as (r_c, θ_c) or in normalized Cartesian coordinates as (f_c, g_c). According to Hopkins theory of partially coherent imaging [21], the + 1st-order spectrum of the aerial image intensity for a binary grating object can be formulated as:

$$I\left[\mathbf{r}_m, J\left(\mathbf{r}_c\right), h\right] = \frac{1}{2\pi}\left\{TCC\left[\mathbf{0}, \mathbf{r}_m; J\left(\mathbf{r}_c\right), h\right] + TCC\left[-\mathbf{r}_m, \mathbf{0}; J\left(\mathbf{r}_c\right), h\right]\right\}. \qquad (1)$$

Here, $\mathbf{r}_m$ is a vector in the pupil plane, which can be expressed in normalized polar coordinates as (r_m, θ_m) corresponding to the pitch and orientation of the binary grating; *TCC* is

#132739 - $15.00 USD Received 2 Aug 2010; accepted 28 Aug 2010; published 3 Sep 2010

transmission cross coefficient given by $TCC\left[\mathbf{r}',\mathbf{r}'';J(\mathbf{r}_c),h\right]=\int_{-\infty}^{+\infty}J(\mathbf{r}_c)H(\mathbf{r}'+\mathbf{r}_c,h)H^*(\mathbf{r}''+\mathbf{r}_c,h)d\mathbf{r}_c$; $H(\mathbf{r},h)$ is the pupil function given by $H(\mathbf{r},h)=\exp\left[-ikW(\mathbf{r},h)\right]\mathrm{circ}(\mathbf{r})$; $k = 2\pi/\lambda$ is the wave number; λ is the wavelength of the monochromatic light source; $W(\mathbf{r},h)$ is the total aberrated wavefront given by $W(\mathbf{r},h)=W_{odd}(\mathbf{r})+W_{even}(\mathbf{r})+h\cdot w_{defocus}(\mathbf{r})$, which includes the lens odd aberration $W_{odd}(\mathbf{r})$, the lens even aberration $W_{even}(\mathbf{r})$, and the defocus aberration that is induced by another even-type aberration $w_{defocus}(\mathbf{r})=\sqrt{1-NA^2|\mathbf{r}|^2}-1$ multiplied by an axial shift h from the ideal focal plane; NA is the image-side numerical aperture of the projection lens.

The impact of odd aberration and even aberration on imaging is to respectively change the phase shift $\varphi[\mathbf{r}_m,J(\mathbf{r}_c),h]$ and amplitude $\left|I\left[\mathbf{r}_m,J(\mathbf{r}_c),h\right]\right|$ of the image intensity spectrum. After through-focus analyzing the + 1st-order spectrum of the aerial image intensity, we can obtain a phase shift value $\varphi[\mathbf{r}_m, J(\mathbf{r}_c)]$ of the + 1st-order spectrum at the ideal focal plane corresponding to $h = 0$, and an axial shift value $h = D[\mathbf{r}_m, J(\mathbf{r}_c)]$ satisfying the condition $\partial\left|I\left[\mathbf{r}_m,J(r_c),h\right]\right|/\partial h=0$ where the amplitude of the + 1st-order spectrum reaches its maximum. Noticing that $\exp\left[-ikW(\mathbf{r},h)\right]=\cos\left[kW(\mathbf{r},h)\right]-i\left[\sin kW(\mathbf{r},h)\right]$ and considering a small amount of aberration $W(\mathbf{r}, h)$ in the lithographic tools, we have approximated formulas $W(\mathbf{r},h)\sim 0$, $\cos\left[kW(\mathbf{r},h)\right]\sim 1$, and $\tan\left[kW(\mathbf{r},h)\right]\sim\sin\left[kW(\mathbf{r},h)\right]\sim kW(\mathbf{r},h)$, thus we can simplify $\varphi[\mathbf{r}_m, J(\mathbf{r}_c)]$ and $D[\mathbf{r}_m, J(\mathbf{r}_c)]$ as [15]:

$$\varphi\left[\mathbf{r}_m,J(\mathbf{r}_c)\right]=\frac{k}{J_0}\int_S J(\mathbf{r}_c)\left[W_{odd}(\mathbf{r}_m+\mathbf{r}_c)-W_{odd}(\mathbf{r}_c)\right]d\mathbf{r}_c, \tag{2}$$

$$D\left[\mathbf{r}_m,J(\mathbf{r}_c)\right]=\frac{1}{J_1}\int_S J(\mathbf{r}_c)\left[W_{even}(\mathbf{r}_m+\mathbf{r}_c)-W_{even}(\mathbf{r}_c)\right]\cdot\left[w_{defocus}(\mathbf{r}_c)-w_{defocus}(\mathbf{r}_m+\mathbf{r}_c)\right]d\mathbf{r}, \tag{3}$$

where $J_0=\int_S J(\mathbf{r}_c)d\mathbf{r}_c$ and $J_1=\int_S J(\mathbf{r}_c)\left[w_{defocus}(\mathbf{r}_m+\mathbf{r}_c)-w_{defocus}(\mathbf{r}_c)\right]^2 d\mathbf{r}_c$; S is the integral region which is determined by the intersection of two different shift pupils and represented in normalized Cartesian coordinates (f_c, g_c) as the shaded area shown in Fig. 1.

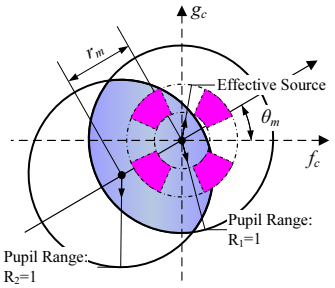

Fig. 1. Representation of the integral region S in normalized Cartesian coordinates.

By expressing the aberration as a series of Zernike polynomials:

$$W_{odd}(\mathbf{r}_m)=\sum_{n\_odd}Z_{n\_odd}R_{n\_odd}(\mathbf{r}_m), \tag{4}$$

$$W_{even}(\mathbf{r}_m)=\sum_{n\_even}Z_{n\_even}R_{n\_even}(\mathbf{r}_m), \tag{5}$$

where $\boldsymbol{R}_n(\mathbf{r}_m)$ indicates the nth Zernike polynomial, n_odd and n_even indicate the Zernike indexes for odd aberration and even aberration respectively, Eqs. (2) and (3) can be written as:

#132739 - $15.00 USD Received 2 Aug 2010; accepted 28 Aug 2010; published 3 Sep 2010

$$\varphi\left[\mathbf{r}_m, J(\mathbf{r}_c)\right] = \sum_{n\_odd} Z_{n\_odd} F_{n\_odd}\left[\mathbf{r}_m, J(\mathbf{r}_c)\right], \tag{6}$$

$$D\left[\mathbf{r}_m, J(\mathbf{r}_c)\right] = \sum_{n\_even} Z_{n\_even} G_{n\_even}\left[\mathbf{r}_m, J(\mathbf{r}_c)\right]. \tag{7}$$

We define $F_{n\_odd}[\mathbf{r}_m, J(\mathbf{r}_c)]$ and $G_{n\_even}[\mathbf{r}_m, J(\mathbf{r}_c)]$ as two sensitivities for odd aberration and even aberration respectively, and they have the formulations of:

$$F_{n\_odd}\left[\mathbf{r}_m, J(\mathbf{r}_c)\right] = \frac{k}{J_0}\int_S J(\mathbf{r}_c)\left[R_{n\_odd}(\mathbf{r}_m + \mathbf{r}_c) - R_{n\_odd}(\mathbf{r}_c)\right] d\mathbf{r}_c, \tag{8}$$

$$G_{n\_even}\left[\mathbf{r}_m, J(\mathbf{r}_c)\right] = \frac{1}{J_1}\int_S J(\mathbf{r}_c)\left[R_{n\_even}(\mathbf{r}_m + \mathbf{r}_c) - R_{n\_even}(\mathbf{r}_c)\right]\cdot\left[w_{defocus}(\mathbf{r}_c) - w_{defocus}(\mathbf{r}_m + \mathbf{r}_c)\right] d\mathbf{r}_c. \tag{9}$$

From Eqs. (8) and (9), each of the odd and even aberration sensitivities has a compact formulation as a function determined by independent variables of the Zernike order, source distribution and pupil position. Although they are quite similar to those derived in our previous paper [15], it is obvious that the newly developed formulations are generalized and suitable for arbitrarily shaped illumination sources with variable intensity distributions. In fact, as we use the partial coherence factor σ to represent a conventional source with a circular top-hat distribution, Eqs. (8) and (9) will be simplified to have the identical formulations shown as Eqs. (20) and (21) in Ref. 15. In addition, with a certain Zernike order, the aberration sensitivity can be treated as an analytical kernel for measuring the corresponding Zernike coefficient. The amount of each analytical kernel with a fixed source distribution will only depends on the position in the pupil plane that is expressed in normalized vector coordinate $\mathbf{r}_m$ or polar coordinates as (r_m, θ_m).

Figures 2 and 3 depict the analytical kernels respectively for measuring the odd and even aberrations from Z_2 to Z_{37} under the smooth conventional illumination shown in Fig. 5. As expected, the analytical kernels have the same symmetric properties along the angle θ_m at a fixed r_m as the corresponding Zernike polynomials do. Therefore, similar to the Zernike polynomials, the analytical kernels can be categorized into $1\theta_m$ kernels (*n_odd* = 2, 3, 7, 8, 14, 15, 23, 24, 34, 35), $3\theta_m$ kernels (*n_odd* = 10, 11, 19, 20, 30, 31), and $5\theta_m$ kernels (*n_odd* = 26, 27) for odd aberrations, together with $0\theta_m$ kernels (*n_even* = 4, 9, 16, 25, 36, 37), $2\theta_m$ kernels (*n_even* = 5, 6, 12, 13, 21, 22, 32, 33), and $4\theta_m$ kernels (*n_even* = 17, 18, 28, 29) for even aberrations.

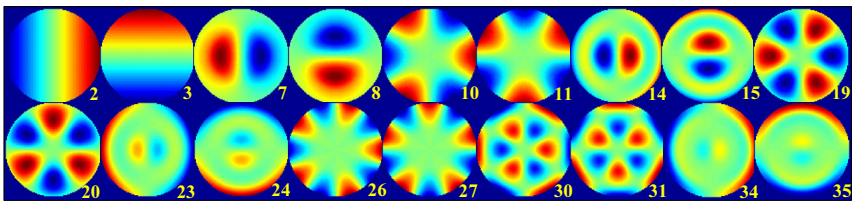

Fig. 2. Characterization of analytical kernels for measuring odd aberrations under the smooth conventional illumination shown in Fig. 5.

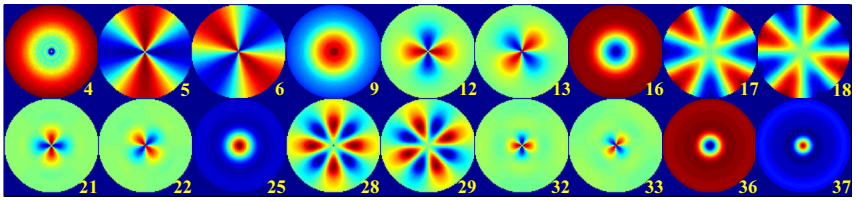

Fig. 3. Characterization of analytical kernels for measuring even aberrations under the smooth conventional illumination shown in Fig. 5.

#132739 - $15.00 USD Received 2 Aug 2010; accepted 28 Aug 2010; published 3 Sep 2010

It is well known that lens aberrations are always modeled mathematically in the pupil plane by the sum of a set of Zernike coefficients multiplying the corresponding Zernike polynomials which are completely orthogonal polynomials over the interior of the unit circle. Hence, the Zernike polynomials build a linear relationship between the aberration and the Zernike coefficients in the pupil plane. According to Eqs. (4) to (7), the proposed analytical kernels act in a similar way in Eqs. (6) and (7) as the Zernike polynomials do in Eqs. (4) and (5), although these kernels containing information of both the pupil and the illumination source are not strictly orthogonal. It is clear that the proposed kernels take the advantage of realizing and achieving a linear and analytical relationship between the Zernike coefficients to be measured and the measurable physical signals $\varphi[\mathbf{r}_m, J(\mathbf{r}_c)]$ and $D[\mathbf{r}_m, J(\mathbf{r}_c)]$, which leads to be not only accurate but also efficient for aberration in-line monitoring under arbitrary illumination sources. If we concentrate on a set of Zernike coefficient from Z_2 to Z_N (N is the highest concerned Zernike order), the corresponding analytical kernels from Z_2 to Z_N are able to together construct a generalized sensitivity function space. As shown in Fig. 4, after obtaining the physical signals from through-focus images by Fourier transform (FT), it is easy to map the $\varphi[\mathbf{r}_m, J(\mathbf{r}_c)]$ and $D[\mathbf{r}_m, J(\mathbf{r}_c)]$ into the sensitivity function space where the weights of corresponding kernel components indicate the Zernike coefficients to be measured, which is the essential physical meaning of linear Eqs. (6) and (7).

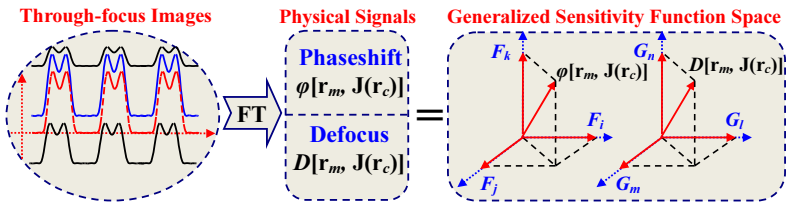

Fig. 4. Expansion of $\varphi[\mathbf{r}_m, J(\mathbf{r}_c)]$ and $D[\mathbf{r}_m, J(\mathbf{r}_c)]$ in the generalized sensitivity function space.

For instance, with a set of 36 binary gratings, two sets of 36 linear equations can be obtained from Eqs. (6) and (7), and expressed in a matrix notation of $\mathbf{\Phi} = \mathbf{F}\mathbf{Z}_{\text{odd}}$ and $\mathbf{D} = \mathbf{G}\mathbf{Z}_{\text{even}}$, where $\mathbf{\Phi}$ and $\mathbf{D}$ are vectors respectively containing the phase shifts and the axial shifts of the + 1st-order intensity spectrums at the setting of 36 binary gratings; $\mathbf{Z}_{\text{odd}}$ and $\mathbf{Z}_{\text{even}}$ are unknown vectors to be measured, and respectively containing the Zernike coefficients for odd aberration and even aberration; $\mathbf{F}$ and $\mathbf{G}$ are two matrixes of sensitivities for measuring odd aberration and even aberration respectively. Since there are more equations than unknowns, both two sets of equations become over-determined and Zernike coefficients form Z_2 up to Z_{37} can be solved by the least-square method.

3. Simulation

We applied the lithographic simulator PROLITH to simulate and demonstrate the overall measurement performance of the proposed technique. The wavelength used in simulation is 193nm with a fixed NA of 0.75. As shown in Fig. 5, different types of illumination sources commonly used in mainstream lithographic tools were introduced as inputs for simulation. The upper row in Fig. 5 shows the smooth sources with variable intensity distributions, including conventional ($\sigma = 0.31$), annular ($\sigma_i/\sigma_o = 0.4/0.7$), dipole ($\sigma_i/\sigma_o$/degree = 0.4/0.7/45°), and quadrupole (σ_i/σ_o/degree = 0.4/0.7/45°) shapes, which were respectively constructed by convolving the corresponding top-hat distribution sources shown in the lower row in Fig. 5 with a Gaussian kernel diffusion length of 0.1 [20].

#132739 - $15.00 USD Received 2 Aug 2010; accepted 28 Aug 2010; published 3 Sep 2010

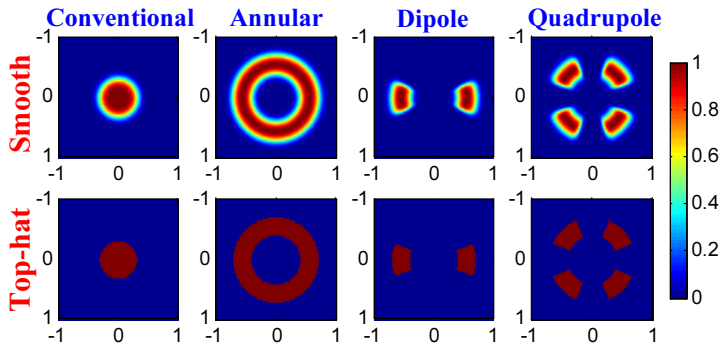

Fig. 5. Representation of mainstream types of illumination sources with different intensity distributions. The upper row: Smooth mainstream illumination sources with a Gaussian blur introduced as inputs for the simulation, including conventional, annular, dipole, and quadrupole shapes. The lower row: Top-hat mainstream illumination sources including conventional, annular, dipole, and quadrupole shapes.

The matrixes of sensitivities F and G obtained by the generalized formulations are critical factors for aberration metrology. For a set of 36 different binary gratings under a certain illumination setting, each of F and G contains 18 × 36 elements of sensitivities. We numerically calculated these sensitivities using the generalized formulations, and subsequently performed comparisons with those simulated by PROLITH. The comparison results for the four smooth sources shown in Fig. 5 are depicted in Figs. 6(a) and 6(b) as two correlation plots respectively for odd aberration sensitivities and even aberration sensitivities. It is observed that the maximum deviations of the odd sensitivities and even sensitivities are 0.0092 and 0.0079, respectively. These excellent correlations validate that the generalized formulations of matrixes F and G are suitable for arbitrarily shaped illumination sources with variable intensity distributions.

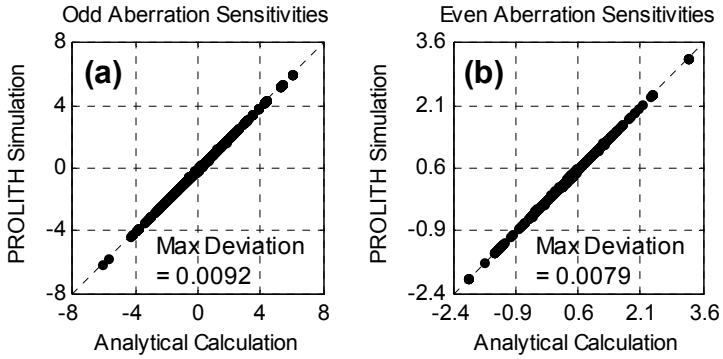

Fig. 6. Correlation plots of aberration sensitivities between analytical calculation and PROLITH simulation for the four smooth sources shown in Fig. 4. (a) For odd aberration sensitivities, and (b) for even aberration sensitivities. Each of (a) and (b) totally contains 4 × 18 × 36 dots for the four input sources.

We performed lots of simulations to further test the accuracy of the proposed technique. As an instance, Figs. 7 and 8 depict the simulation result for the smooth quadrupole illumination shown in Fig. 5. Here four aberrated wavefront values with Zernike coefficients from Z_2 up to Z_{37} were used as inputs for the simulation. The comparison between the input and measured aberrated wavefronts is illustrated in Fig. 7. It is clear that the measured wavefront values are in good agreement with the input ones with absolute measurement errors less than 3.5mλ. Figure 8 shows the measurement errors of individual Zernike coefficients from Z_2 up to Z_{37} for the input aberrated wavefront 1. The upper chart represents a comparison of the input Zernike coefficients and the measured values, and the lower chart

#132739 - $15.00 USD Received 2 Aug 2010; accepted 28 Aug 2010; published 3 Sep 2010

represents the absolute errors of Zernike coefficients. The measured values of the Zernike coefficients are noted to coincide quite closely with the input values. From the simulation result, the absolute errors of all Zernike coefficients are less than 0.62mλ. From this observation and lots of other simulation results for different arbitrarily shaped sources, it is found that the proposed technique yields a superior quality of wavefront estimate with an accuracy on the order of mλs and accuracy of Zernike coefficients on the order of 0.1mλs.

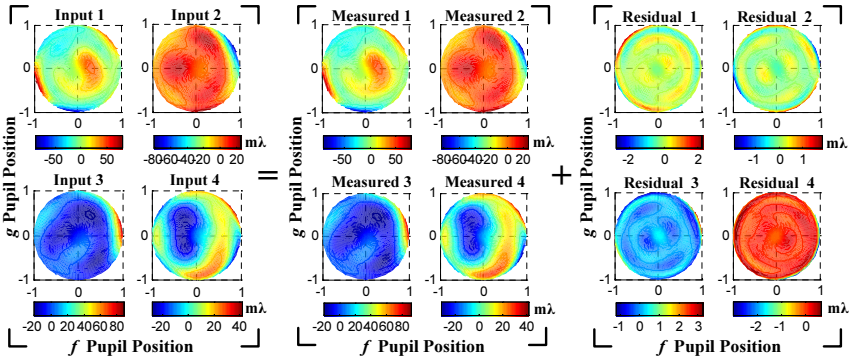

Fig. 7. Comparison between the input and measured aberrated wavefronts under the smooth quadrupole illumination shown in Fig. 5.

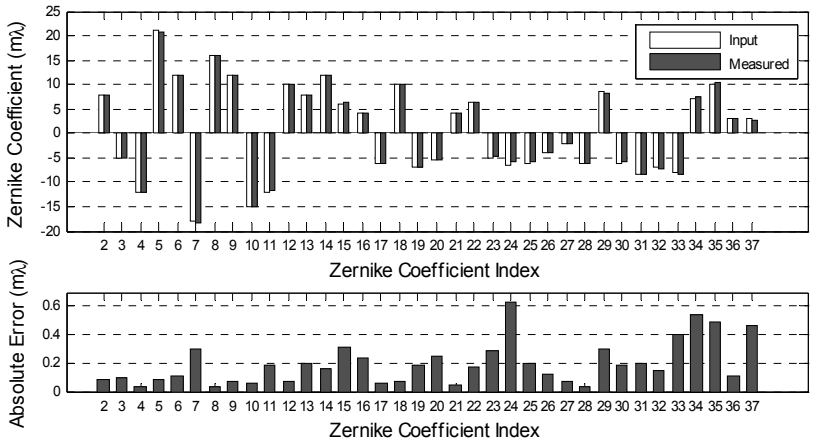

Fig. 8. Simulation results of the measurement errors of Zernike coefficients for the input aberration 1 under the smooth quadrupole illumination shown in Fig. 5.

In our technique the Zernike coefficients solved by the least-square method rely heavily on the two matrixes of sensitivities **F** and **G**, which are determined directly by the effective source function $J(\mathbf{r}_c)$ together with the set of binary gratings $\mathbf{r}_m$ (i.e., pupil sampling scheme). It is promising to enhance the overall performance by optimizing either of the effective source function, the pupil sampling scheme, or both of them. It is also interesting to note that if we obtain the aerial image intensities with only several fixed binary gratings but at multiple illumination source and NA settings, our technique will be quite similar to the commonly used TAMIS technique [8]. From this point of view, our technique can be considered as a generalized one that provides more flexible configurations for wavefront metrology.

4. Conclusion

A generalized technique is proposed for in situ metrology of lens aberrations up to the 37th Zernike coefficient in lithographic tools, suitable for arbitrarily shaped illumination sources with variable intensity distributions. The technique is presented in a compact form with

#132739 - $15.00 USD Received 2 Aug 2010; accepted 28 Aug 2010; published 3 Sep 2010

generalized formulations of odd and even aberration sensitivities which can be treated as a set of analytical kernels corresponding to a set of concerned Zernike orders. The analytical kernels succeed in realizing a linear and analytical relationship between Zernike coefficients and the measurable physical signals under arbitrarily shaped illumination sources. A variety of mainstream illumination sources with spatially variable intensity distributions were input into the PROLITH to conduct the simulation work. According to the simulation results, the proposed technique has been proved to be simple in implementation and yield a superior quality of wavefront estimate, hence it is expected to provide a useful practical means for the in-line monitoring of imaging performance of current lithographic tools.

Acknowledgements

This work was supported by National Natural Science Foundation of China (Grant No. 91023032, 51005091, 50775090) and Program for New Century Excellent Talents in University of China (Grant No. NCET-06-0639). The authors would like to thank National Engineering Research Center for Lithographic Equipment of China for the support of this work and KLA-Tencor Corporation for providing an academic usage product of PROLITH™ software.

#132739 - $15.00 USD Received 2 Aug 2010; accepted 28 Aug 2010; published 3 Sep 2010